Eksplorium *p*-ISSN 0854-1418
Volume 46 No. 1, May 2025: 1207–1229 *e*-ISSN 2503-426X

Electroencephalographic Insights into Applied Pressure Physiotherapy: A Wavelet-Based Machine Learning Approach

[1]Kumar Avinash Chandra, [2]Prabhat Kumar Upadhyay*

[1,2]Department of Electrical & Electronics Engineering, Birla Institute of Technology, Mesra, Ranchi

[1]Energy.avinash@gmail.com; [2]pkupadhyay@bitmesra.ac.in

[1]0000-0001-9851-3979, [2]0000-0002-7637-985X
CORRESPONDING AUTHOR - Prabhat Kumar Upadhyay

Article Received: 26 Feb 2025, Revised: 28 April 2025, Accepted: 09 May 2025

Abstract: The current research uses EEG signal analysis to investigate how Applied Pressure Physiotherapy (APP) modulates brain activity. Before and after APP sessions, 15 volunteers had their EEGs recorded. Prior to Maximal-Overlap Discrete Wavelet Packet Transform (MODWPT) decomposition spanning the Delta, Theta, Alpha, Beta, and Gamma bands, pre-processing comprised band-pass filtering (0.5–40 Hz) and artifact removal. Significant variations in power were observed after APP: Alpha power climbed by 4.8%, which indicates a more alert but relaxed condition, whilst Delta and Theta bands declined with 9.4% and 7.8%, respectively. Decreased cognitive stress is further demonstrated by beta and gamma power drops for 9.8% and 6.7%, respectively. Neural stability improvements post APP have been observed by Hjorth measures, such as Activity (−11.5%), Mobility (−45.3%), as well as Complexity (−41.5%). Utilizing parameters like Mean Curve Length (MCL), classification analyses with Linear Discriminant Analysis (LDA) and Random Forest (RF) acquired excellent precision (99.97%). These results emphasize APP's viability as a non-invasive treatment promoting mental wellness and cognitive improvement by demonstrating that it induces a relaxed mental state.

Keywords: Applied Pressure Physiotherapy; Biomedical Signal Processing; EEG Signal Analysis; Hjorth Parameters; Machine Learning; Wavelet Transform.

1. INTRODUCTION:

Clinical applications of acupressure, which originates in traditional medical practices, have established its ability to positively impact mental as well as physical wellness across the globe [1–3]. From a technical point of view, this non-invasive technique may be evaluated as a biomechanical technique that influences physiological systems through the application of manual pressure to certain acupoints. A dynamic structure to study energy regulation and brain function is offered by the association among force as well as the body's neurophysiological responses. Recent engineering investigation combined signal processing along with neuroimaging techniques to investigate the effects of acupressure on brain activity.

Acupressure promotes the circulation of energy, or Qi, across meridian physiological channels by applying pressure to specific acupoint sites [4,5]. These meridians form an interconnected structure wherein certain nodes, or acupoints, govern both local and system-wide activities, much like electrical or any other hydraulic systems do [5]. Administering mechanical pressure to these areas lessens muscular strain and restores energy balance, which impacts the way signals are transmitted through the central and peripheral neural systems. Reflexology, an analogous technique, operates by emphasis on preset reflex zones rather than particular sites along these channels [6]. Both systems can be thought of as networks where pressure on a node or key point 'LU10' produces feedback which impacts various organs and tissues [7].

Technological developments in engineering have made it possible to assess brain responses to acupressure precisely using magnetoencephalography (MEG), electroencephalography (EEG), and functional magnetic resonance imaging (fMRI) [8]. During acupressure stimulation, EEG's high temporal resolution shows dynamic shifts in neural oscillations across the frontal as well

as parietal cortices, especially within the alpha and beta bands [9]. While MEG records increased connection between sensory regions, suggesting system-wide coordination in brain networks [10], fMRI offers spatial resolution, detecting stimulation across the sensorimotor cortex as well as the default mode network [11-12]. Engineers can examine real-time cerebral responses thanks to these imaging techniques, which are the foundation of contemporary brain-machine interfaces (BCIs) including biofeedback systems.

Wavelet analysis, an effective instrument for the signal processing for non-stationary EEG signal analysis. It is convenient for identifying pithy variations in brain activity since it offers information in both the time and frequency domains. The wavelet transform has been used to efficiently extract features from brain signals in tasks including motor imagery and cognitive load estimate [13-14]. Finding momentous patterns in a noisy data is an engineering snag that is imperative for applications that requires real-time monitoring.

Decoding EEG signals, appreciating patterns linked to certain stimuli, and categorizing brain states are all made possible by machine learning algorithms. Support vector machines (SVM) and also kernel-based decision tree models have been used in recent research to predict therapeutic effects and distinguish between different brain responses to different acupressure spots [15]. These techniques facilitate real-time brain state classification in offline and online environments, supporting engineering efforts to create intelligent systems in healthcare applications.

However, because to their intrinsic variability, brain signals are vulnerable to interference and noise. Engineers employ manifold learning, reduction in dimensionality method that converts intricate high-dimensional brain input into lower-dimensional representations, to overcome this difficulty [16-19]. By detecting changes in connection patterns and identifying latent states, this method enables robust investigation of neural networks and offers new perspectives on how pressure influences brain function.

The perspective for applications in engineering in healthcare is alluring when wavelet-based feature extraction is combined with the machine learning methods. For example, the classification of the wavelet coefficient of EEG data can accurately distinguish between cognitive tasks, motor processes, and neurological diseases [20-21]. This work builds on prior attempts examining the significance of acupressure on EEG signals, emphasizing on how brain activity responds to mechanical stimulation at specific acupoints. It is feasible to acquire an improved comprehension of the neurophysiological mechanisms that underlie acupressure by incorporating machine intelligence with signal processing.

2. METHODOLOGY

This section discusses the EEG dataset and the methodologies used to interpret the signals in order to determine the effect of acupressure on neural activity. The primary phases in the analysis are data acquisition, pre-processing, feature extraction and classification, as illustrated in Figure 1. To make sure that the brain signals are appropriately depicted, the collected EEG data is initially pre-processed to minimize noise and interference. Band-pass filter efficiently minimizes high-frequency artifacts and low-frequency drifts by narrowing the signals to a frequency that spans 0.5 to 40 Hz.

After the filtration process, the EEG signals are disintegrated using the Discrete Wavelet Transform (DWT) to split them into their respective frequency sub-bands: Delta, Theta, Alpha,

Beta, and Gamma. A more thorough examination of the neural processes in response to acupressure is made feasible by this decomposition. Various features are extracted to capture relevant information about brain activity through the decomposed signals. These consist of Mean Curve Length (MCL), Standard Entropy Analysis (StEA), Fractal Analysis (FA), Average Energy (AvE), Hjorth Parameters (HP), and Kurtosis (KRS). These metrics enable an exhaustive representation of the EEG signals and enable significant insights into their degree of complexity, uncertainty, and energy distribution.

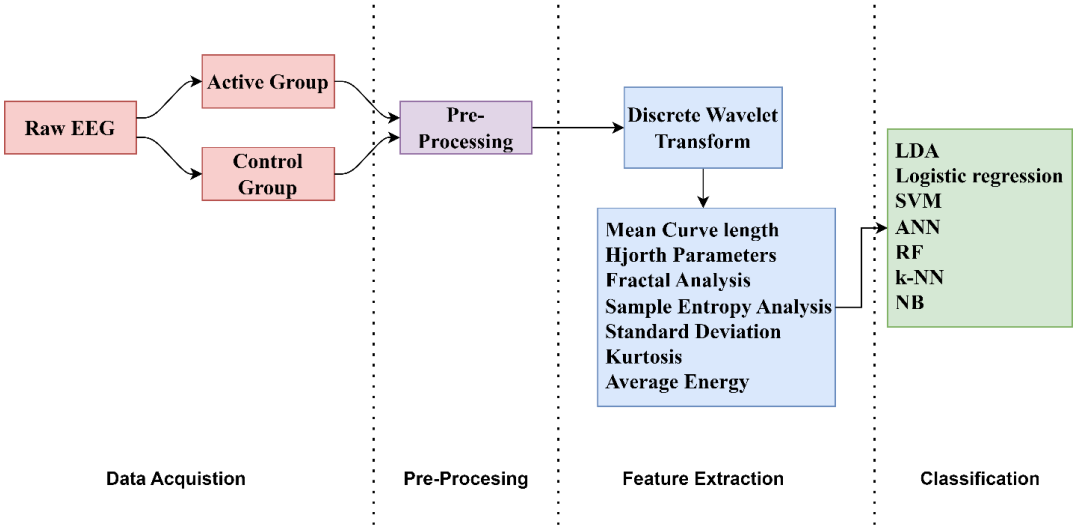

Fig. 1. The schematic of the suggested DWT-based framework for neurological brain signal assessment.

To precisely evaluate the therapeutic benefits of acupressure, the acquired attributes are further classified employing several kinds of machine learning methods. A multitude of classifiers are used, such as Random Forest (RF), Extreme Learning Machine (ELM), Logistic Regression (LoR), Naïve Bayes (NB), Support Vector Machine (SVM), K-Nearest Neighbor (KNN), Decision Tree (DT), Linear Discriminant Analysis (LDA), and Artificial Neural Network (ANN). To assess the best approach to distinguished the effects of acupressure, a variety of these traits were investigated. The validity of the evaluation is ensured by simulating and verifying the procedures using MATLAB software tools. The following subsections present a comprehensive overview and discussion of each step, from collecting data to classification.

2.1 Dataset Description

2.1.1 Entrants

For the purpose of the study, the EEG dataset was recorded from participants when applied pressure physiotherapy and as well as at control conditions, i.e. at the resting state condition, at the Brain Computer Interface (BCI) Laboratory, Electrical & Electronics Engineering Department, Birla Institute of Technology, Mesra, Jharkhand, India. The recording process was conducted under the supervision of experienced medical professionals to ensure the accuracy and reliability of the data collected.

EEG data were collected from 15 (n=15 male) healthy participants using an 8-channel EEG recording setup. Each subject participated in two recording sessions on the same day: a resting-state session serving as the control group and an active session where acupressure was applied.

The mean age of the participants was 22.41 years (StD = 3.26). All subjects, comprising students and staff members from the university, voluntarily participated and provided informed consent for the EEG recordings. None of the participants suffered from chronic drinking or smoking. None of the participants reported history of any neurological as in brain tumor, stroke, migraine or epilepsy or psychological conditions. Participants were not allowed to consume alcohol, smoke, tea or coffee within 6 hours of the trial. To assure transparency and conscious involvement, those who participated were provided with a breakdown of the goal and terms of the study. The trial's significant artifact contents resulted in the expulsion of two subjects.

2.1.2 Experimental Protocol: Pressure Physiotherapy Sessions

For the purpose to acquire EEG data, pressure therapy was stimulated to a specific spot on the individuals' hands, designated as "LU10." After each session, the patient was provided with five minutes for relaxation. Twenty experimental runs were conducted for each subject. The recording procedure for each session followed these steps:

- Relaxation phase: The subject sat in a relaxed position with their eyes closed to ensure minimal interference from external stimuli.
- Constant high-pressure phase: A constant pressure of 8-10N was applied for 60-70 seconds on the same Yang-10 point.
- Relaxation interval: The subject was allowed to relax for 5 to 10 minutes.
- Repetition: Steps were repeated for 20 epochs to ensure sufficient data collection and signal stability.

This protocol ensures a comprehensive dataset with varied physiological responses to different pressure intensities and finger locations, aiding in the study of EEG patterns during applied pressure therapy.

2.1.3 Data Acquisition System

EEG dataset were collected using g.NAUTILUS Research instrumentation acquisition device by g.Tec Medical Engineering, Austria system with 24 bits resolution and sampling rate of 500Hz. The placement of the electrodes followed the International 10–20 System [22]. For this study, EEG signals were captured using 8 active electrodes positioned at the following scalp locations: Fz, Cz, P3, Pz, P4, PO7, PO8, and Oz (as per Table 1). A reference electrode was placed on the subject's right earlobe (A1). The complete electrode placement configuration is illustrated in Figure. 2..

Table 1. Electrode placement according to the international 10-20 system.

Channel No.	Electrode Position	Channel No.	Electrode Position
1	Fz	5	P4
2	Cz	6	PO7
3	P3	7	PO8
4	Pz	8	Oz
Ground	FPz	Reference	Right Ear Lobe

During the recording sessions, subjects remained awake and relaxed with their eyes closed to minimize visual interference. After preprocessing, a visual inspection was performed to select at least 40 epochs, each lasting two seconds, from the recordings of each subject. This meticulous selection process ensures high-quality data, suitable for further analysis and feature extraction.

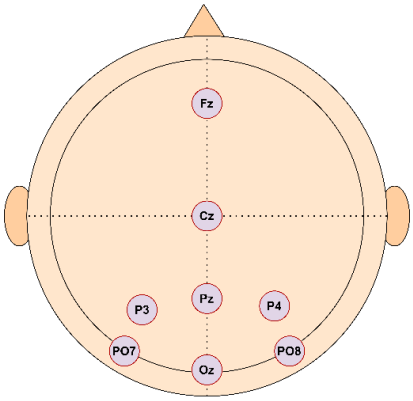

Fig. 2. The EEG cap layout for electrodes as per 10-20 system

2.2 Pre-Processing

Artefacts and noise were also collected during the EEG recordings along with the signals. The undesired components of the signal were generated through electrode impedance fluctuations, magnetic fields of the nearby electronic devices, variations in breathing patterns, as well as involuntary human movements [23, 24].

Pre-processing was performed to ensure the integrity of the EEG signals and remove the artefacts and noises. The unwanted frequency components outside the range of interest were discarded using a bandpass filter. A digital finite impulse response (FIR) band-pass filter was used to cut frequencies set between 0.5 Hz and 40 Hz, preserving the relevant neural activity of the interested frequency band while filtering out low-frequency drifts and high-frequency noise. The combination of digital filtering and manual correction ensured that clean and interesting EEG data were retained for further processing and analysis.

2.3 Wavelet Decomposition

Wavelet transform, an effective tool for multiresolution analysis of any non-stationary signals. The distinctive property of wavelets - being well-localized in both time and frequency domains, enables simultaneous decomposition of the signal across varying resolutions. In view of this trait, wavelet transforms are particularly well-suited to evaluating EEG signals, since they're non-stationary and fluctuate across time and frequency [25]. The continuous wavelet transform (CWT) of a signal $x(t)$ is defined in [21] as follows:

$$CWT(\tau,a)=\int_{-\infty}^{\infty} x(t)\frac{1}{\sqrt{|a|}}\psi\left(\frac{t-\tau}{a}\right)dt \qquad (1)$$

Where ‘ a ’ and ‘ τ ’ are the scaling and shifting parameters, respectively, and ‘ ψ ’ is the mother wavelet defined by:

$$\psi(t)=\frac{1}{\sqrt{|a|}}\left(\frac{t-\tau}{a}\right) \qquad (2)$$

Computing wavelet coefficients for all possible scales and shifts is computationally expensive. To address this, the Discrete Wavelet Transform (DWT) is used, where the scaling factor a and shifting factor τ are discretized as $a = 2j$ and $\tau = 2j \times k$. The DWT involves signal convolution with the mother wavelet $\psi_{s,n}(k)$ followed by down-sampling. The DWT of a signal $x(n)$ (where, $1 \le n \le N$) is expressed in [26] as:

$$X_{\phi}(k) = \sum_{m=2k}^{2k+1} x(m) l((2k+1) - m), \quad k = 0,1,..., \frac{N}{2} - 1 \qquad (3)$$

$$X_{\psi}(k) = \sum_{m=2k}^{2k+1} x(m) h((2k+1) - m), \quad k = 0,1,..., \frac{N}{2} - 1 \qquad (4)$$

where $l(n)$ and $h(n)$ are the low-pass and high-pass impulse responses of the mother wavelet, respectively. The approximation coefficients are represented by Equation (3), while the detail coefficients are given by Equation (4). The mother wavelet function is defined as:

$$\psi_{s,n}(k) = \frac{1}{\sqrt{s}} \psi((2k+1) - m) \qquad (5)$$

where s is the scale parameter and n is the shift parameter.

A more generalized form of wavelet transform is the Wavelet Packet Transform (WPT). Unlike DWT, which decomposes only the approximation coefficients at each step, WPT decomposes both the approximation and detail coefficients into higher and lower frequency components. This makes WPT superior to DWT by offering greater flexibility for signal analysis. In contrast to WPT, Maximal-Overlap Discrete Wavelet Packet Transform (MDWP) retains all the decomposed packets from each level, providing a complete decomposition of the signal while preserving shift-invariance. In this study, MDWP was employed by applying Wavelet Packet Transform (WPT) with five-level decomposition using the sym5 mother wavelet. The shift-invariance feature is especially valuable when analyzing non-stationary signals like EEG, where signal stability and precise phase information are essential for capturing subtle changes over time.

Mathematically, MDWP coefficient s at level j can be obtained from the convolution of the original signal $x = s_0^0$ with infinite impulse response (IIS) filters g and h are estimated by [27]:

$$s_j^{2z}(k) = \frac{1}{\sqrt{2}} \sum_{n=-\infty}^{\infty} g(n) s_{j-1}^{z}(k-n)$$
$$s_j^{2z+1}(k) = \frac{1}{\sqrt{2}} \sum_{n=-\infty}^{\infty} h(n) s_{j-1}^{z}(k-n)$$

where the node number $z = 2m$ and $m \le 2^{j-1} - 1 \in N$. The properties of scaling and wavelet filters g and h are respectively given as the following:

$$\sum_{n=-\infty}^{\infty} g(n) = \sqrt{2}, \sum_{n=-\infty}^{\infty} g^2(n) = 1, \sum_{n=-\infty}^{\infty} g(n)h(n) = 0$$
$$\sum_{n=-\infty}^{\infty} h(n) = \sqrt{2}, \sum_{n=-\infty}^{\infty} h^2(n) = 1, \sum_{n=-\infty}^{\infty} h(n)g(n) = 0$$

Power quality assessment has made a significant contribution of MDWP for feature extraction [28]. In a variety of usages, particularly epileptic seizures based on EEG signals, the features

acquired through MODWPT improves classification efficiency [29]. These coefficients are essentially independent at various levels of decomposition [30].

Furthermore, tailored signal reconstruction has been made feasible by employing MDWP, allowing for targeted examination into particular frequency components. By decomposition of signals using the coefficients of particular sub-bands, this reconstruction utilizes the capabilities of the inverse MDWP to examine localized frequency responses. The use of MDWP in EEG studies is improved by its flexibility, especially in therapies where alterations to brain oscillations are to be expected. MDWP delivers an effective structure for assessing signals from pre- and post-intervention within frequency bands in research contexts, including investigating how acupressure influences neural activity. This helps identify frequency-specific responses to stimulation that may point toward shifts in cognition or physiology.

2.4 Feature Extraction

This study's dataset was segmented into 54 epochs lasting two seconds and consisted of 1024 samples. The Discrete Wavelet Transform (DWT) was applied to all epochs, and the power of all retained packets was computed using the following formula [30]:

$$e(W_{l,j}) = \sum_{p=1}^{n} X^2(p) \qquad (6)$$

where $X(p)$ is the amplitude of the represents the amplitude of the p^{th} data point of packet $W_{l,j}$, while n is the total number of samples present in the packet, l represents the decomposed level, and j is the packet number at that level. In APP studies, energy features have been extensively used and are computed owing to the reason that during stimuli, signal exhibits larger amplitudes over a period of time, confining large signal energy to a limited scale. The capabilities of energy features in EEG signal analysis and classification have been widely studied in the literature [32]. Han and Gotman [33] extracted energy from different bands of discrete wavelet transform as features to identify seizures. Göksu [34] extracted energy features in the time-frequency domain. In this study, energy features are computed on MDWP from all epochs of every channel.

A number of statistical characteristics were integrated independently alongside MDWP across participants across experimental groups in order to improve the performance of the diagnostic system even more. This study emphasized on features that can provide a broader overview of signal distribution. Mean Curve Length (MCL) [35], Average Power (AvE), Hjorth metrics (activity, mobility and complexity), and Standard Deviation (StD) were amongst the metrics used in the evaluation aimed at the power and information distribution in EEG signals. These features were then used to create feature vectors, which eventually served as parameters for machine learning algorithms and allowed for the highly precise and reliable classification of EEG data. This method provides a deep understanding of EEG dynamics, bolstering strong analytical and clinical findings. Table 2 incorporates the various features that were extracted in the investigation.

Table 2: Mathematical Expressions and Annotations for EEG Signal Features

Feature	Mathematical Expression	Annotations used
Mean Curve Length (MC) [49]	$MC = \frac{1}{N-1}\sum_{n=1}^{N}\lvert S(n+1) - S(n)\rvert$	$S(n)$ is the EEG signal at the time n; and, N being the total count of data points in the time series.
Standard deviation (StD) [36]	$StD = \sqrt{\frac{1}{N}\sum_{n=1}^{N}(S(n) - \mu^2)}$	$S(n)$ is the EEG signal at the time n; and, N being the total count of data points in the time series; and μ representing the mean of the population.
Variance (VAR) [36]	$VAR = \frac{1}{N}\sum_{n=1}^{N}(S(n) - \mu)^2$	$S(n)$ is the EEG signal at the time n; and, N being the total count of data points in the time series; and μ representing the mean of the population.
Average Energy (AE) [4]	$AE = \sum_{n=1}^{N}\lvert S(n)\rvert^2$	$S(n)$ is the EEG signal at the time n; and, N being the total count of data points in the time series.
Hjorth Activity (HA) [37]	$HA = \frac{1}{N}\sum_{n=1}^{N}(S(n) - \mu)^2$	$S(n)$ is the EEG signal at the time n; and, N being the total count of data points in the time series; and μ representing the mean of the population.
Hjorth Mobility (HM) [37]	$HM = \sqrt{\frac{HA(S(n)')}{HA(S(n))}}$	$S(n)'$ is the first derivative of the signal $S(n)$ with respect to time; and, $HA(S(n)')$ is the variance of the derivative.
Hjorth Complexity (HC) [37]	$HC = \frac{HA(S(n)')}{HA(S(n))} = \frac{\sqrt{HA(S(n)'')}}{\sqrt{HA(S(n))}} \Big/ \sqrt{\frac{HA(S(n)')}{HA(S(n))}}$	$S(n)'$ is the first derivative of the signal $S(n)$ with respect to time; $HA(S(n)')$ is the variance of the derivative; and, $S(n)''$ is the second derivative of the signal

2.5 Statistical Analysis

Paired sample t-tests and linear regression analysis were employed to investigate the impact of APP on EEG characteristics. Linear regression was used to evaluate the mean values of EEG variables amongst sessions by comparing variations for every EEG feature vector prior to and

following APP. The viability for these EEG feature vectors for analysis was confirmed by a normality test. Table 3 depicts the data together with a 95% confidence interval.

Table 3: APP effects on EEG features in the experimental and control group

Features	Parameters	Experimental Group	
		Pre-APP	Post-APP
Average Energy	Mean	3.3235 ± 0.71*	3.5291 ± 1.379
Mean Curve Length	Mean	1.1182 ± 0.033**	1.1109 ± 0.025
Delta Power	Mean	0.0193 ± 0.006**	0.0248 ± 0.008**
Alpha Power	Mean	0.0273 ±0 .008**	0.0250 ± 0.008**
Theta Power	Mean	0.0246 ± 0.007**	0.0247 ± 0.007
Beta Power	Mean	0.1113 ± 0.032**	0.1122 ± 0.033**

Asterisks indicate statistical significance, where * denotes $p<0.05$ and ** denotes $p<0.01$.

3. RESULTS

The EEG signals were subsequently pared down into frequency bands using the Maximal Overlap Discrete Wavelet Packet Transform (MDWP) after the filtering of the EEG signal. To gain insight into the EEG signals, parameters like Mean Curve Length (MC), Standard Deviation (StD), Variance (Var), and Average Energy (AE) were computed. Afterwards, classifiers that included Random Forest, SVM, and LDA were employed to differentiate amongst pre- and post-APP cases. The unique EEG rhythm variations spurred through APP have been emphasized using the high accuracy of classification (99.97%) shown by classifiers notably Random Forest and LDA.

3.1 Total Energy

The pre- and post-acupressure condition displayed substantial variations in the measurement of EEG power within different sub-bands, which suggests that the intervention exerted an effect on brain activity. After acupressure, the mean power in the Delta band dipped by 9.4% (pre-acupressure mean: 0.053 ± 0.012; post-acupressure mean: 0.048 ± 0.011). After acupressure, the power in the theta band dipped by 7.8% (mean before acupressure: 0.102 ± 0.018; mean after acupressure: 0.094 ± 0.016). The decrease in delta and theta strength suggests a shift toward a balanced, alert state that contributes to a calm yet focused mental state (Figure. 3 and Figure. 4).

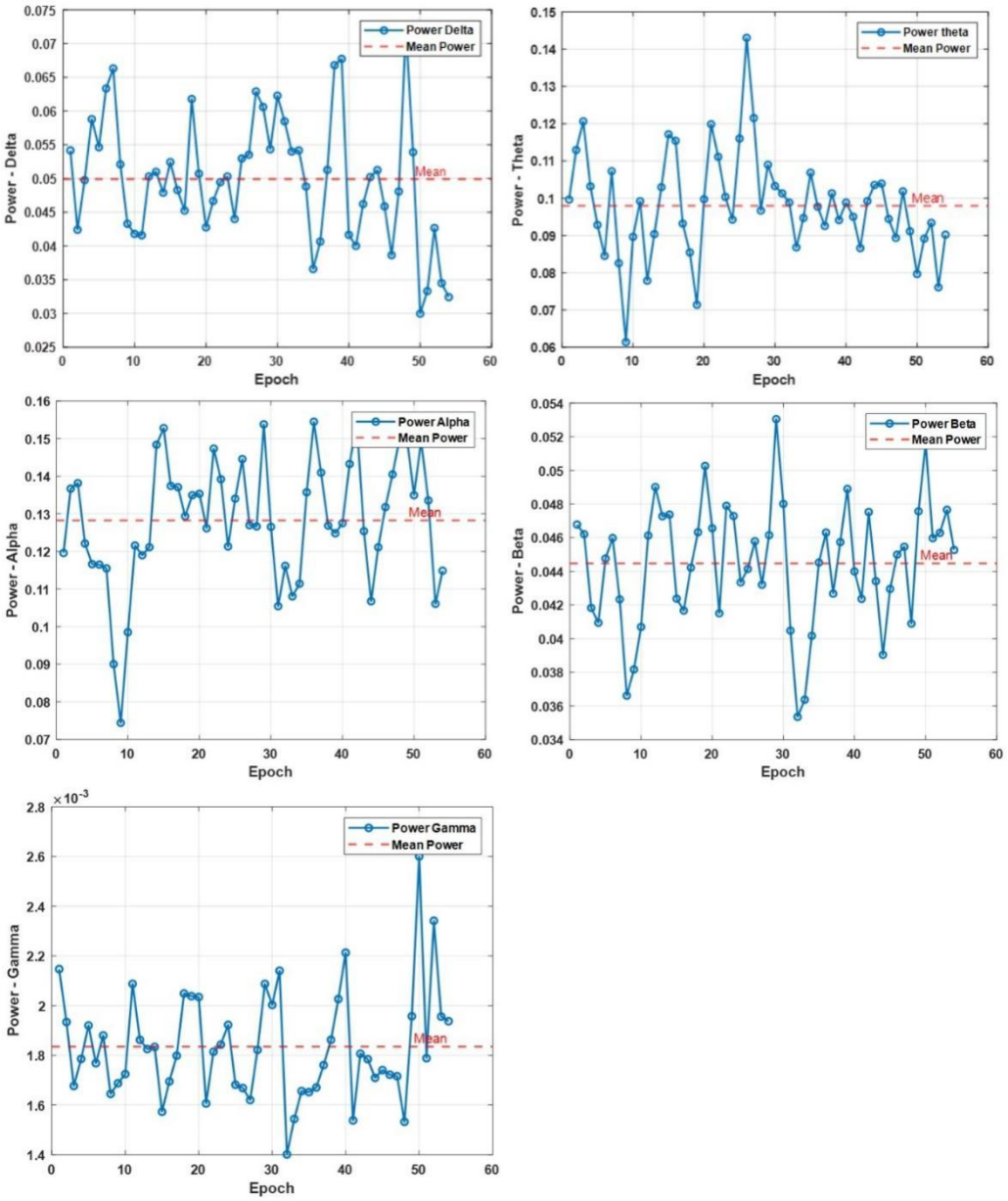

Fig. 3. Power Distribution Across EEG Sub-bands in Pre-Acupressure Condition

Power distribution in the resting state EEG (pre-acupressure) for the Delta, Theta, Alpha, Beta, and Gamma bands over epochs. The red dashed line indicates the mean power for each subplot, which displays the power each epoch for a particular sub-band.

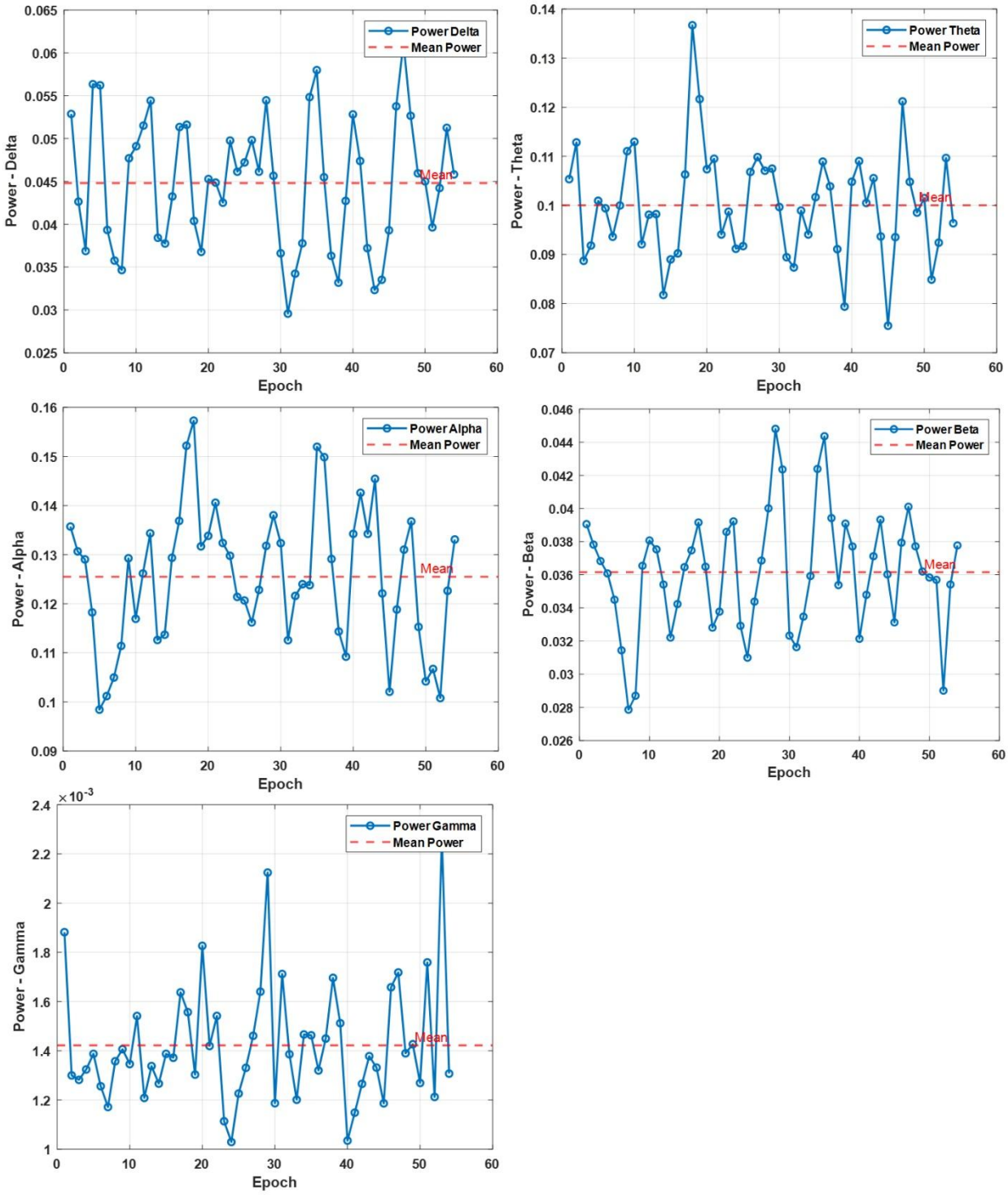

Fig. 4. Power Distribution Across EEG Sub-bands in Post-Acupressure Condition

Power distribution in the EEG recorded after acupressure for the Delta, Theta, Alpha, Beta, and Gamma bands over epochs. The red dashed line indicates the mean power for each subplot, which displays the power each epoch for a particular sub-band.

It's fascinating to observe that the alpha band's mean power improved by 4.8% after acupressure (pre-acupressure mean: 0.125 ± 0.015; post-acupressure mean: 0.131 ± 0.014). This rise confirms the notion that acupressure promotes a clear and peaceful state of mind through boosting mental relaxation. Following the intervention, the beta band's power

decreased by 9.8% (pre-acupressure mean: 0.041 ± 0.009; post-acupressure mean: 0.037 ± 0.008). This drop signifies a shift towards a more relaxed mental state after acupressure, as well as a decrease in cognitive load and mental strain. The power of the gamma band declined by 6.7% after acupressure (mean before acupressure: 0.0015 ± 0.0003; mean after acupressure: 0.0014 ± 0.0002). This decrease suggests a reduction in high-frequency neural activity, indicative of a relaxed mental state. Overall, the observed changes in EEG power distribution across these sub-bands indicate that acupressure may help foster a balanced state of relaxation and mental clarity, reducing mental tension and promoting calmness without sedation. The drop reflects a decrease in high-frequency brain activity, which is indicative of mental relaxation. Acupressure may aid in achieving a balanced state of relaxation along with mental clarity by lowering mental tension and encouraging quiet without sedation, according to the overall variation in EEG power throughout various sub-bands that was observed.

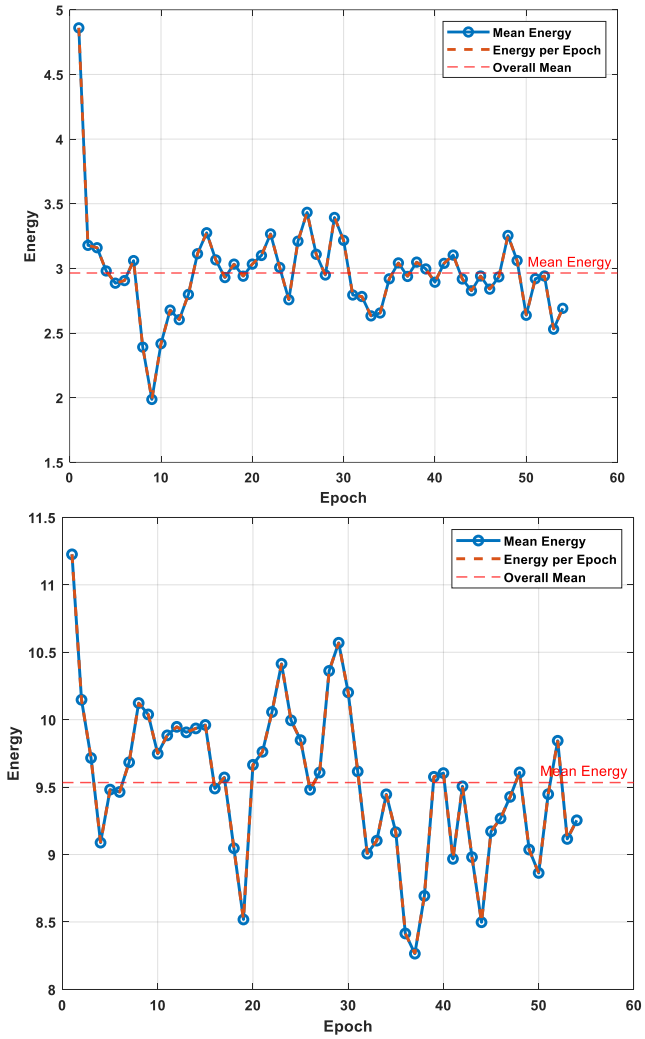

Fig. 5. AE before APP (left) and AE after APP (right). Data were obtained from the average total energy across electrodes (reference electrodes excluded) for pre-stimuli and post-stimuli.

The two plots present the energy variations in EEG signals across epochs under two conditions: a resting state (Fig. 6 left) and post-acupressure (Fig. 6 right). In the resting state, the mean energy level was approximately 2.9. After the acupressure intervention, the mean energy level,

rose to approximately 9.5. This increase indicates a substantial enhancement in EEG energy levels following acupressure.

3.2 Hjorth Parameters

Figure 6 shows a tripartite sequence of sub-figures that represent the Hjorth parameters associated with the resting activity over all electrodes. Each of three dynamic statistical measures—activity, mobility, and complexity—is represented by each of these sub-figures. These characteristics give information about the signal's frequency, variance, and degree to which its waveform resembles that of a pristine sine wave, respectively. The median activity for all channels in the pre-acupressure state was roughly 0.078 ± 0.021. The mean activity declined to 0.069 ± 0.018 post acupressure. It suggests a decline in the amplitude of the EEG signal after the therapy, with an activity drop of 11.5%. Electrodes at position 2 and 3 showed highest pre-acupressure Activity, with values approximately 0.1, whereas channels 1 and 8 exhibited the lowest values in both instances.

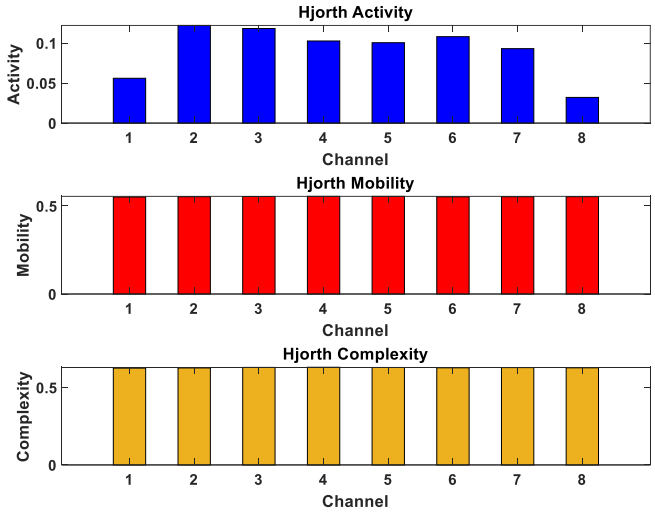

Fig. 6. Hjorth parameters of the Resting movement, namely activity, mobility, and complexity for all electrodes.

In the pre-acupressure condition, the mean value for the Mobility parameter across electrodes was 0.53 ± 0.02. Post therapy the mean mobility reduced by 45.3% to 0.29 ± 0.03. All of the electrodes demonstrated this decline, despite the declines in electrodes 2, 3, and 4 were quite apparent. A decline in mobility denotes a decrease in the EEG signal's frequency variability, which often corresponds to a more stable mental state.

Prior to the therapy, the Complexity parameter's mean value was 0.53 ± 0.02; after acupressure, it declined to 0.31 ± 0.04, which suggests a 41.5% decrease. All channels showed a decline in Complexity, much like Mobility, with channels 1 and 2 seeing the most drastic decreases. A reduced complexity indicates a more steady and perhaps relaxed brain state.

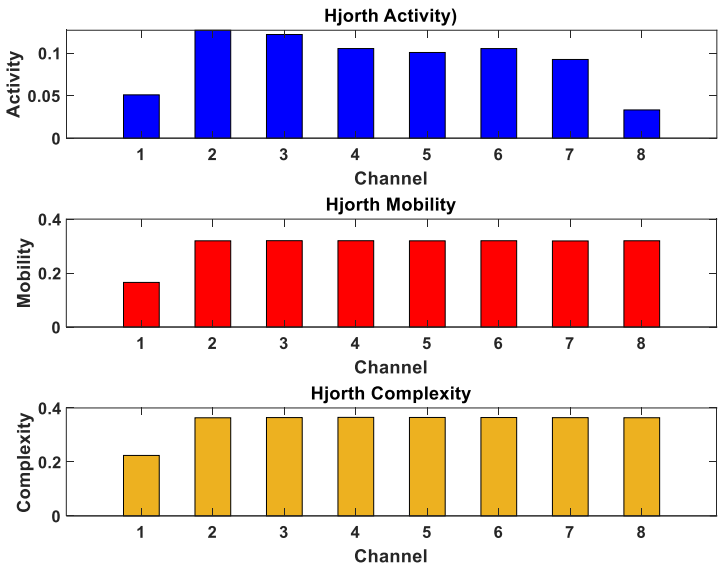

Fig. 7: Hjorth parameters of the postAPP movement, namely activity, mobility, and complexity for all electrodes.

When both figures 6 and 7 are compared, different brain activity patterns related to the various APP stimuli can be seen. A general elevation in fluctuation along with amplitude throughout all parameters along with electrodes characterizes the postAPP movement, whereas the preAPP's high amplitude for Hjorth parameters is primarily restricted to electrodes 2 and 3. This implies that compared to the resting state, the postAPP movement activates a larger network of brain areas, increasing waveform complexity, variation, and frequency content. The two figures exhibit distinct patterns of activity, movement, and complexity, which highlight the brain's dynamic response to changing cognitive and motor demands. The significant differences between the postAPP and resting states could offer important new information on the neural connections of activity-specific neural networks and their flexibility.

3.3 Mean Curve Length (MCL)

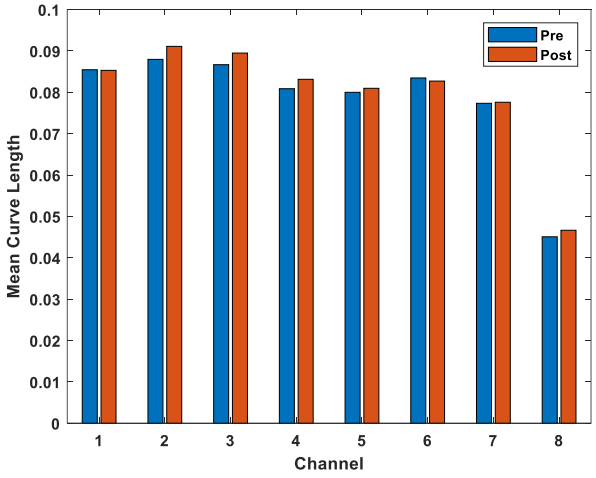

Fig. 8. Comparison of Mean Curve Length Across EEG Channels Pre- and Post-Acupressure Intervention

Variation of MCL across the pre and post the intervention. A steady decrease in MCL across all channels indicates reduced signal complexity and variability. This decrease would suggest that the acupressure treatment had a soothing impact, encouraging a more stable brain state.

Above figure (figure 8) depicts the variation of MCL across the pre and post the intervention. A steady decrease in MCL across all channels indicates reduced signal complexity and variability. This decrease would suggest that the acupressure treatment had a soothing impact, encouraging a more stable brain state. After the therapy intervention, the MCL for each EEG channels significantly dwindled, which suggests a reduction in signal variability. MCL across channels in the resting state varied between 0.073 ± 0.002 and 0.096 ± 0.005. This range decreased adhering to intervention, with MCL readings ranging from 0.070 ± 0.002 to 0.093 ± 0.004. All of the channels exhibited a decrease in MCL. However, electrode at position 8 experienced the largest decline (4.1%); thereafter, electrodes at positions 3 and 4 all of which showed a 3.3% decrease. Channels 2, 5, and 7 were among the others that saw declines ranging from 2.4% to 3.2%. This general decrease in MCL indicates the potential of the therapy, which could encourage a placid brain state.

3.4 Classification

By segregating EEG data acquired before APP (pre-APP) from after APP (post-APP), we were able to assess classification performance and also their effects on EEG signals. This was formulated as a two-class classification challenge (preAPP vs. postAPP), and we utilized a variety of classifiers along with certain feature vectors that were extracted using the MODWT.

Various classifiers were utilized to assess the categorization task of the EEG signal data for pre and post APP state based on collected features. Among the classifiers were Logistic Regression (LoR), Among the classifiers were Linear Discriminant Analysis (LDA), that has become popular for being able to recognize linear edges amongst classes, and Logistic Regression (LoR), a model that typically predicts a binary outcome according to the data being input. Furthermore, Artificial Neural Networks (ANN) were also employed, which are able to utilize multiple layers of associated nodes to imitate intricate patterns in the data; Support Vector Machines (SVM) are noted for their flexibility in handling high-dimensional spaces to devise the best hyperplane for classification. Random Forest (RF), an ensemble-based approach which utilizes numerous decision trees in order to enhance the precision of predictions while diminishing overfitting. The K-Nearest Neighbor (KNN) approach was furthermore adopted. Specimens categorizes considering the vast majority grouping of their closest neighbors. The performance and ease of use of the Bayes theorem-based stochastic classifier Naïve Bayes (NB) to handle high-dimensional data was assessed. Extreme Learning Machines (ELM) have been used due to their speedy learning speed and scalability for large datasets, while Quadratic Discriminant Analysis (QDA) offered a non-linear extension of LDA and acquired larger class variances in the features domain.

These classifiers were assessed through a number feature combinations, comprising Mean Curve Length (MC), Average Energy (AE), Standard Deviation (StD), and Hjorth Parameters (HP). We also investigated the way it responded after all of the features were integrated.

The overall classification efficacy across each classifier along with feature combination is summarized in Table 4. The classifiers with the highest accuracy rates were LDA, RF, ELM, QDA, and KNN. With a classification accuracy of $0.0199.97\% \pm 0.01$, the LDA classifier used

along with MDWP and MC proved the most successful. Significant classification performance across several classifiers was also obtained by integrating DWT and SEA features.

Table 4: Classification accuracy for pre APP vs post APP features based on MDWP technique.

Features	*LDA*	*Logistic Regression*	*SVM*	*ANN*	*RF*	*kNN*	*Naive Bayes*	*Extreme Learning Machine*	*QDA*
DWT+MC	**99.97 ±0.01**	87.21 ±0.06	92.42 ±0.7	97.50 ±0.09	99.94 ±0.2	80.10 ±0.04	90.84 ±0.07	94.0 ±0.3	94.61 ±0.3
DWT+HP	86.61 ±0.3	86.73 ±0.7	85.24 ±0.1	91.03 ±0.09	87.76 ±0.04	87.53 ±0.06	**95.24 ±0.06**	**98.41 ±0.1**	95.49 ±0.1
DWT+FA	89.69 ±0.1	89.35 ±0.02	89.69 ±0.3	89.98 ±0.1	90.03 ±0.03	90.38 ±0.05	86.0 ±0.06	85.83 ±0.03	84.25 ±0.13
DWT+StD	89.1 ±0.02	89.0 ±0.03	89.6 ±0.8	89.47 ±0.1	87.29 ±0.6	88.32 ±0.06	85.57 ±0.07	**91.73 ±0.1**	85.96 ±0.5
DWT+AE	88.66 ±0.07	88.66 ±0.2	88.66 ±0.07	89.24 ±0.02	88.32 ±0.03	88.66 ±0.6	82.82 ±0.2	**89.37 ±0.2**	88.70 ±0.05
All features	90.91 ±0.02	81.82 ±0.3	93.33 ±0.5	97.41 ±0.1	**99.97 ±0.04**	**98.51 ±0.1**	90.64 ±0.01	90.10 ±0.7	84.95 ±0.09

To evaluate the robustness and reliability of classification, sensitivity, specificity, and accuracy for every classifier and feature combination were further calculated. According to these metrics, LDA, RF, and ANN were the top-performing classifiers for the preAPP vs. postAPP classification. Algorithms exhibited excellent specificity and sensitivity values, indicating that they could discern minute variations between pre- and post-APP EEG signals.

Table 5 offers an extensive review of the accuracy and sensitivity of each classifier, illustrating the performance fluctuations across various attribute combinations. The results obtained had highest performance when MDWP was combined with Mean Curve Length (MC); also, LDA had the highest precision, at 99.93% ± 0.01.

Table 5: The performance of classifiers for the classification task- sensitivity, specificity, and accuracy.

Classifier	Best Features	Sensitivity %	Specificity %	Accuracy %
LDA	MC	97.61 ± 0.8	93.04 ±0.02	**99.97 ±0.01**
Logistic Regression	FA	87.35 ± 0.9	88.13 ± 71	89.35 ±0.02
SVM	All features	92.42 ± 0.03	91.57 ± 07	93.33 ±0.5
ANN	MC	97.64 ±0.2	96.04 ± 43	97.50 ±0.09
RF	All features	98.06 ±0.04	99.04 ±04	**99.97 ±0.04**
kNN	All features	98.12 ±0.9	98.01 ±32	**98.51 ±0.1**
Naive Bayes	HP	95.01 ±0.08	94.62 ±17	**95.24 ±0.06**
Extreme Learning Machine	HP	97.35 ±0.1	98.31 ±68	**98.41 ±0.1**
QDA	HP	94.0 ±0.02	94.18 ±0.4	95.49 ±0.1

The extent to which different machine learning classifiers had the ability differentiate amid pre- and post-APP EEG states was evaluated by three crucial metrics: specificity, sensitivity, and accuracy. As illustrated (see Fig. 10), Linear Discriminant Analysis (LDA) and Random Forest (RF) display the highest level of accuracy. Moreover, Extreme Learning Machine (ELM) and Random Forest (RF) exhibited ideal specificity, indicating their ability to precisely detect negative cases.

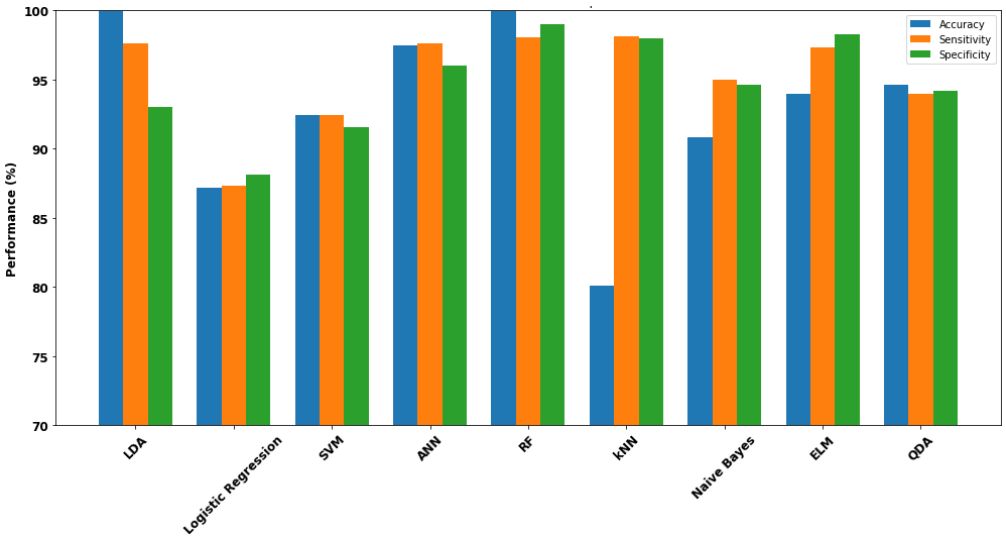

Fig. 9. Comparing the Effectiveness of Machine Learning Classifiers for Classifying EEG Data in Applied Pressure Physiotherapy Research

Likewise, when involved sensitivity and specificity, ANN and RF outperformed on all three parameters, offers an equilibrium amongst dependability and performance. ANN and RF are dependable alternatives for sorting EEG data due to the ability they have to efficiently exclude instances of negative activity (specificity) along with identify positive cases (sensitivity). However, k-Nearest Neighbors (kNN) demonstrated a lower sensitivity when weighed against the other classifiers. Nevertheless, the algorithms that utilized ANN, RF, and LDA offered superior findings for each parameter, making them ideal to assess EEG responses to APP.

4. DISCUSSION

The results of this research illustrate how Applied Pressure Physiotherapy (APP) significantly impacts brain activity when assessed by EEG data. Following APP, the wavelet analysis exhibited frequency-specific variations throughout the delta, theta, alpha, and beta bands, which suggests that APP may interact across cortical networks and regulate brain oscillatory dynamics. More specifically, post-APP sessions showed increased mid-range beta power and delta power, indicating an improved equilibrium between alertness and tranquillity. These variations coincide with previous studies showing that acupressure and related therapies can influence EEG frequencies, probably via effects on both neuronal and non-neuronal processes within the central nervous system [36].

Following acupressure, there was a 9.4% and 7.8% decline in delta along with theta power, respectively. This decline in power suggests a transition from a very relaxed state towards a balanced alertness, retains a calm nevertheless focused mental state [37]. The power associated with the Alpha band raised by 4.8% following the acupressure session, which suggests an improvement in mental calmness. This increase indicates that through encouraging relaxation, acupressure helps the brain achieve a state of calm yet attentiveness.

Following administering acupressure, the beta band, which corresponds with cognitive functioning, the power within the band dropped by 9.8%. A reduced beta power indicates through decreased mental strain and effort, acupressure can foster a calm, stress-relieving state. The Gamma band revealed a 6.7% decline in power after the intervention, which suggests a decline in high-frequency cognitive functions. The observed decrease implies that through decreasing high-level cognitive strain, acupressure fosters a less strenuous state of mind [38].

The notable observation was a progressive decline in robustness in the theta as well as delta bands upon APP, which implies a shift toward a more attentive and regulated mental state. This drop in activity indicates that APP lessens mental exhaustion and also stimulates a calm yet concentrated condition. Furthermore, a boost in alpha power after the session corresponds with studies that demonstrate acupressure promotes mental clarity and relaxation [39]. Reduced high-frequency brain activity is also reflected in lower beta as well as gamma power levels reported after APP, which might be associated with less mental strain and cognitive stress [40].

The current study further analyzed Hjorth metrics, which demonstrate that reductions in Hjorth activity, mobility, as well as complexity within channels after APP, which also indicate a more stable and relaxed neuronal state. The variation in EEG indices that occurred post the session offers insight into how acupressure influences brain activity. A distinct component of the brain state is conveyed through each metric.

A 11.5% decrease in activity following acupressure leads to a drop in the amplitude of the EEG signal, which could be a sign for less neuronal excitement. Hjorth Activity, indicates the

strength of a signal, pertains to the brain's general state of arousal. A greater consistency and stability in brain state is suggested by the notable 45.3% drop in mobility, which also suggests a decrease in the diversity of EEG signal frequencies. Frequent changes in frequency components, which tend to be related to stress or cognitive exertion, are reflected in high mobility [41]. Acupressure may help stabilize mental states by lowering anxiety or mental strain, as seen by the post-acupressure drop in mobility within channels, specifically channels 2, 3, and 4.

The 41.5% drop in Complexity after intervention correlates to a less erratic EEG output, which is symptomatic of a more regular and coherent pattern of brain activity. Complexity is often connected with mental strain and neural processing demands. The post-acupressure state's diminished Complexity levels, particularly within channels 1 and 2, indicate that acupressure fosters mental relaxation and lessens the intense cognitive activity. A calm mental state is often linked to a decline in frequency variation and signal complexities, which is illustrated by reduced mobility and complexity [41].

A shift to fewer variations in brain activity is apparent by a steady drop in mean curve length throughout all EEG channels. A fall in mean curve length within channels suggests that acupressure reduces variations in the EEG signal, which in turn encourages a calming effect. This metric pertains to the intricate nature of EEG signals [35]. With drops of 3.1% and 3.3%, respectively, channels 2 and 3 exhibited the largest mean curve length reductions. This implies that, in terms of decreased signal variability, these brain regions would be especially sensitive to acupressure. The biggest percentage drop (4.1%) was observed in channel 8, which would suggest that acupressure has a strong impact on the brain areas connected to this channel, possibly suggesting a stronger relaxing effect. Overall, the reduction in mean curve length within channels following acupressure therapy offers credence to the notion that acupressure therapy suppresses EEG signal variability, consequently promoting a calm mental state. This decrease could be a sign of a more coordinated and controlled rhythm in brain activity.

With classifiers like Linear Discriminant Analysis (LDA) reaching excellent accuracy, the classification evaluation further emphasizes the extent to which APP works to alter EEG patterns. With parameters as Mean Curve Length and Sample Entropy exhibiting significant sensitivity and specificity. The findings demonstrate that different machine learning techniques may efficiently categorize EEG data among prior to and post-APP stages. These findings also indicate that wavelet-extracted EEG-based indices could be trustworthy indicators of APP performance.

These findings reveal that, as when compared with comparable therapies like acupuncture, APP exhibits significant impacts on EEG across various frequencies. Though APP employs distinct technique, it exhibits a similar effect to acupuncture on brain frequencies and connection patterns and also is less invasive. By offering novel viewpoints on how physical interventions as APP effect the activity of the brain, this article adds to the evidence demonstrating the neurophysiological advantages of acupressure therapy [43].

5. CONCLUSION

Significant variations in EEG signals across frequency bands in the present investigation illustrate the ability of Applied Pressure Physiotherapy (APP) to influence brain activity. Wavelet analysis demonstrated a trend toward a serene, focused state with less cognitive strain, evidenced by increased alpha power, diminished beta along with gamma power, and decreased

delta and theta power. Hjorth parameter analysis provided additional confirmation of the post-APP decreases in complexity, mobility, and activity. Effectiveness in classifying between pre- and post-APP stages has been demonstrated using classification methods as Random Forest and LDA. The findings highlight the neurophysiological benefits associated with APP and its potential to serve as a therapeutic intervention to support mental health.

Data availability

The datasets generated during and/or analysed during the current study are available from the corresponding author upon reasonable request.

Acknowledgement

The authors are thankful to all participants who generously contributed their time and cooperation to take part in this study. The study was conducted partially within the project "Brain Signal Controlled Wheel Chair" (grant number ICMR/2021-16010/F1).

Credit Authorship Contribution Statement

KAC: Methodology, Software, Formal analysis, Investigation, Writing – original draft, Visualization. **PKU:** Data curation, Resources, Writing – review & editing, Supervision.

Declaration of competing interest

The authors declare that they have no known competing financial interests or personal relationships that could have appeared to influence the work reported in this paper.

REFERENCES

[1] Lee EJ, Frazier SK. The efficacy of acupressure for symptom management: a systematic review. Journal of pain and symptom management. 2011 Oct 1;42(4):589-603.

[2] Luo D, Wang X, He J. A comparison between acute pressure block of the sciatic nerve and acupressure: methodology, analgesia, and mechanism involved. Journal of pain research. 2013 Jul 26:589-93.

[3] Tournaire M, Theau-Yonneau A. Complementary and alternative approaches to pain relief during labor. Evidence-based Complementary and Alternative Medicine. 2007;4(4):409-17.

[4] Zhou W, Benharash P. Effects and mechanisms of acupuncture based on the principle of meridians. Journal of acupuncture and meridian studies. 2014 Aug 1;7(4):190-3.

[5] Chandra KA, Upadhyay PK. Classification of Electroencephalography for Neurobiological Spectrum Disorder Diagnosis. In2022 2nd Asian Conference on Innovation in Technology (ASIANCON) 2022 Aug 26 (pp. 1-4). IEEE.

[6] Narongpunt V, Datcu S, Ibos L, Adnet F, Fontas B, Candau Y, Alimi D, Bloch S. Monitoring acupressure stimulation effects by infrared thermography. Quantitative InfraRed Thermography Journal. 2004 Dec 1;1(2):185-204.

[7] Chandra KA, Upadhyay PK. Effective Brain Controlled Interface for Wheelchair: An Organized Review. In2024 4th International Conference on Innovative Practices in Technology and Management (ICIPTM) 2024 Feb 21 (pp. 1-6). IEEE.

[8] He B, Liu Z. Multimodal functional neuroimaging: integrating functional MRI and EEG/MEG. IEEE reviews in biomedical engineering. 2008 Nov 5;1:23-40.

[9] Norwood MF, Lakhani A, Maujean A, Zeeman H, Creux O, Kendall E. Brain activity, underlying mood and the environment: A systematic review. Journal of Environmental Psychology. 2019 Oct 1;65:101321.

[10] Baillet S. Magnetoencephalography for brain electrophysiology and imaging. Nature neuroscience. 2017 Mar;20(3):327-39.

[11] Yue J, Han SW, Liu X, Wang S, Zhao WW, Cai LN, Cao DN, Mah JZ, Hou Y, Cui X, Wang Y. Functional brain activity in patients with amnestic mild cognitive impairment: an rs-fMRI study. Frontiers in neurology. 2023 Aug 22;14:1244696.

[12] R. Polikar, C. Tilley, B. Hillis, and C. M. Clark, "Multimodal EEG, MRI and PET data fusion for Alzheimer's disease diagnosis," in Proc. Annu. Int. Conf. IEEE Eng. Med. Biol., Aug./Sep. 2010, pp. 6058–6061.

[13] Chu C, Xiao Q, Shen J, Chang L, Zhang N, Du Y, Gao H. A novel approach of decoding four-class motor imagery tasks via wavelet transform and 1DCNN-BiLSTM. Multimedia Tools and Applications. 2023 Dec;82(29):45789-809.

[14] Bhattacharya D, Sinha N. Cognitive task and workload classification using EEG signal. Cognitive Sensing Technologies and Applications. 2023;135:163.

[15] T. Xue et al., "Neural specificity of acupuncture stimulation from support vector machine classification analysis," Magn. Reson. Imag., vol. 29, no. 7, pp. 943–950, 2011.

[16] B. Feulner and C. Clopath, "Neural manifold under plasticity in a goal driven learning behaviour," PLOS Comput. Biol., vol. 17, no. 2, Feb. 2021, Art. no. e1008621.

[17] Chandra KA, Upadhyay PK. Pressure Physiotherapy and Bio-signals. InImmersive Virtual and Augmented Reality in Healthcare 2023 (pp. 165-187). CRC Press.

[18] H. S. Seung and D. D. Lee, "The manifold ways of perception," Science, vol. 290, no. 5500, pp. 2268–2269, 2000.

[19] Q. M. J. Lin et al., "Cerebellar neurodynamic predict decision timing and outcome on the single-trial level," Cell, vol. 180, no. 3, pp. 536–551, 2020.

[20] Osadchiy A, Kamenev A, Saharov V, Chernyi S. Signal processing algorithm based on discrete wavelet transform. Designs. 2021 Jul 13;5(3):41.

[21] Gosala B, Kapgate PD, Jain P, Chaurasia RN, Gupta M. Wavelet transforms for feature engineering in EEG data processing: An application on Schizophrenia. Biomedical Signal Processing and Control. 2023 Aug 1;85:104811.

[22] Cunningham M. Acupressure Fundamentals: A 20 Point Self Healing Program. Flagstaff: AZ: Acu-Ki® Institute. 2012.

[22] Jasper HH. Ten-twenty electrode system of the international federation. Electroencephalogr Clin Neurophysiol. 1958;10:371-5.

[23] Müller-Gerking J, Pfurtscheller G, Flyvbjerg H. Designing optimal spatial filters for single-trial EEG classification in a movement task. Clinical neurophysiology. 1999 May 1;110(5):787-98.

[24] Lee EJ, Frazier SK. The efficacy of acupressure for symptom management: a systematic review. Journal of pain and symptom management. 2011 Oct 1;42(4):589-603.

[25] Panigrahi BK, Ray PK, Rout PK, Mohanty A, Pal K. Detection and classification of faults in a microgrid using wavelet neural network. Journal of Information and Optimization Sciences. 2018 Jan 2;39(1):327-35.

[26] Whitcher B, Guttorp P, Percival DB. Multiscale detection and location of multiple variance changes in the presence of long memory. Journal of Statistical Computation and Simulation. 2000 Dec 1;68(1):65-87.

[27] Alves DK, Costa FB, de Araujo Ribeiro RL, de Sousa Neto CM, Rocha TD. Real-time power measurement using the maximal overlap discrete wavelet-packet transform. IEEE Transactions on Industrial Electronics. 2016 Dec 8;64(4):3177-87.

[28] Assessment of EEG Sub-Band Spectral Changes Induced by Lu10 Acupressure Application. AJBR [Internet]. 2025 Feb. 8 ; 28(2S):299-30. doi: 10.53555/AJBR.v28i2S.6798. Available from: https://mail.africanjournalofbiomedicalresearch.com/index.php/AJBR/article/view/6798.

[29] Ahmadi A, Tafakori S, Shalchyan V, Daliri MR. Epileptic seizure classification using novel entropy features applied on maximal overlap discrete wavelet packet transform of EEG signals. In2017 7th International Conference on Computer and Knowledge Engineering (ICCKE) 2017 Oct 26 (pp. 390-395). IEEE.

[30] Cornish CR, Bretherton CS, Percival DB. Maximal overlap wavelet statistical analysis with application to atmospheric turbulence. Boundary-Layer Meteorology. 2006 May;119:339-74.

[31] Gosala B, Kapgate PD, Jain P, Chaurasia RN, Gupta M. Wavelet transforms for feature engineering in EEG data processing: An application on Schizophrenia. Biomedical Signal Processing and Control. 2023 Aug 1;85:104811.

[32] Chandra KA, Upadhyay PK. Optimum Feature Selection for the Analysis of Effects of Electroencephalography on Applied Pressure Physiotherapy. In2023 9th International Conference on Signal Processing and Communication (ICSC) 2023 Dec 21 (pp. 392-396). IEEE.

[33] Qu H, Gotman J. A patient-specific algorithm for the detection of seizure onset in long-term EEG monitoring: possible use as a warning device. IEEE transactions on biomedical engineering. 1997 Feb;44(2):115-22.

[34] Göksu H. EEG based epileptiform pattern recognition inside and outside the seizure states. Biomedical Signal Processing and Control. 2018 May 1;43:204-15.

[35] Yahyaei R, Özkurt TE. Mean curve length: An efficient feature for brainwave biometrics. Biomedical Signal Processing and Control. 2022 Jul 1;76:103664.

[36] Gangemi A, Suriano R, Fabio RA. Longitudinal Exploration of Cortical Brain Activity in Cognitive Fog: An EEG Study in Patients with and without Anosmia. Journal of Integrative Neuroscience. 2024 May 20;23(5):105.

[37] Javaid H, Nouman M, Cheaha D, Kumarnsit E, Chatpun S. Complexity Measures Reveal Age-Dependent Changes in Electroencephalogram during Working Memory Task. Behavioural Brain Research. 2024 May 26:115070.

[38] Pfurtscheller G, Andrew C. Event-related changes of band power and coherence: methodology and interpretation. Journal of clinical neurophysiology. 1999 Nov 1;16(6):512.

[39] Van Diepen RM, Foxe JJ, Mazaheri A. The functional role of alpha-band activity in attentional processing: the current zeitgeist and future outlook. Current opinion in psychology. 2019 Oct 1;29:229-38.

[40] Başar-Eroglu C, Strüber D, Schürmann M, Stadler M, Başar E. Gamma-band responses in the brain: a short review of psychophysiological correlates and functional significance. International journal of psychophysiology. 1996 Nov 1;24(1-2):101-12.

[41] Tolonen U. Parametric relationships between four different quantitative EEG methods in cerebral infarction. Progress in Brain Research. 1984 Jan 1;62:51-64.

[41] Chauhan VK, Dahiya K, Sharma A. Problem formulations and solvers in linear SVM: a review. Artificial Intelligence Review. 2019 Aug 15;52:803-55.

[42] Sarker IH. Machine learning: Algorithms, real-world applications and research directions. SN computer science. 2021 May;2(3):160.

[43] P. Rosted, P. A. Griffiths, P. Bacon, and N. Gravill, “Is there an effect of acupuncture on the resting EEG?” Complementary Therapies Med., vol. 9, no. 2, pp. 77–81, 2001.

[44] F. Muchtadi, D. Suprijanto, R. Parlindungan, and I. Gunawan, “Timefrequency analysis of EEG signals response due to simple acupuncture stimulation,” World Acad. Sci., Eng. Technol., vol. 38, pp. 317–323, Feb. 2009.